INVERSE IDENTIFICATION OF HEAT FLUX IN DRY DRILLING PROCESS USING PARTICLE SWARM OPTIMIZATION

José Carlos Medeiros, jose.medeiros.98@gmail.com[1]
Joel Martins Crichigno Filho, joel.crichigno@udesc.br[1]

[1]Santa Catarina State University – UDESC, 200 Paulo Malschitzki St, North Industrial Zone, Joinville, SC

Abstract. **Abstract**. *The dry drilling process presents a major challenge due to the high temperature values. A finite element model created on Abaqus is used to simulate the temperature on the workpiece. This model considers the hole already machined and a move source of heat. The heat flux to the workpiece is modeled as non-uniform in space and time. In this study, experimental tests are conducted on 1020 SAE steel workpiece and the temperatures are measured at different points. The inverse procedure based on particle swarm optimization (PSO) is used to minimize the error between the measured and simulated temperatures. The coefficients of the heat flux to workpiece and the associated error are presented.*

Keywords*: dry drilling, PSO, FEM, heat flux*

1. INTRODUCTION

The heat flux generated in machining and the consequent temperature increases in the workpiece, tool and chip are dependent of the cutting parameters. The prediction of the magnitude and distribution of heat flux allows the correct choice of cutting parameters. This is very important in engineering applications, due to the fact that it allows reducing costs, to improve the manufacturing efficiency and to increase the process quality.

The variation of the temperature can cause thermal deformation of the workpiece. Therefore, the amount of heat that flows into the workpiece it is hard to quantify. The direct identification trough experimental tests are not so simple, due to the errors and the necessity of repeating the experiments. Sometimes the identification by the experimental test is not even possible.

This is very problematic in dry drilling due to the fact the lack of a cutting fluid that would dissipate a part of the heat generated in the process. The development of a finite element model that correctly predicts the heat input in this kind of process could be applied in a lot of engineering applications.

The heat generated on machining process was one of the first and most researched topics in machining. Taylor (1907) was one of the first researches to recognize the importance of heat in accelerating tool wear and he developed an empirical relationship between the cutting speed and the tool life. Ber and Goldblatt (1989) also showed the influence of the temperature in tool's life. He pointed out that a large temperature gradient results in a smaller rate as well as low level of the crate wear.

In general, to calculate the heat flux on machining, it is assumed that almost all the mechanical energy generated during the cutting process is transformed into heat. The Figure 1 shows a model of three different heat generation regions in the cutting zone. In the primary heat zone or shear zone the heat is generated due to plastic deformation that occurs in the chip formation. In the secondary heat zone or tool-chip interface and tertiary heat zone or tool-workpiece interface heat is generated mainly due to friction between the bodies in contact. However it is hard to determine the amount of heat that is transferred to the tool, chip and workpiece. The literature shows that the heat input to workpiece fluctuates massively. The heat input is estimated at 10 - 35% to some authors but due to the wide parameter range, no regularities could be established and that is not possible to determine the workpiece heat input based on the cutting energy (Fleischer et al., 2007).

The determination of the temperature distributions it's very important, because of this a sort of different experimental techniques have been applied to the measurement of machining temperature. However, it is very difficult to achieve good accuracy. The interferences in temperature measurement during a machining process can be caused for a lot of different factors and these interferences can be enough to change the temperature distribution that would have been obtained without any interference. Because of the challenges in the experimental techniques, different methods of calculating the machining temperature have been employed in order to identify the temperature distribution in the cutting process. The various methods of calculating machining temperature may be broadly classified into the following categories: the moving heat source method; the method of image sources; the finite difference method; semi-analytical methods; and the finite element method (Tay, 1993).

Tay et al. (1974) was one of the first to use the finite element method to compute the temperature distribution in the tool, chip and workpiece in orthogonal cutting process. Their approach to calculate the distribution of heat sources was to use the strain-rate and the flow stress distribution. Flow stress was considered as a function of strain, strain-rate and velocity that were calculated from deformed grid patterns obtained from quick-stop experiments. The authors were able to obtain an acceptable complete two-dimensional temperature distribution. Although the method was an accurate method of calculating machining temperature distributions, the necessity of various experiments turns the method in a laborious process.

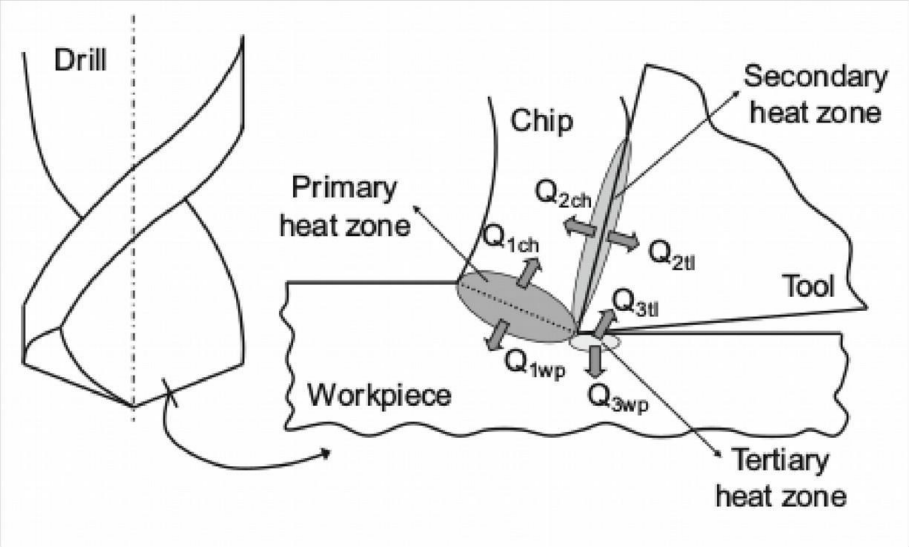

Figure 1: Different heat generation zones (Segurajauregui and Arrazola, 2015)

Bono and Ni (2002) developed a model to predict the heat flow to workpiece in dry drilling. The study used a two-dimensional, axisymmetric finite element model of the workpiece, created on Abaqus. As the drill moves into the workpiece, heat flux is applied to the elements located directly beneath the cutting edge. The drill geometry and the measured drilling thrust and torque are used as input to calculate the heat flux loads. This model only considers the heat flux generated on the chip formation zone.

Biermann and Iovkov (2013) performed a simulation of the drilling process as a transient 3D-analysis. The machined region of the workpiece was implemented with the help of volume segments. They used a two-stage simulation to calculate the heat input, in the first stage the volume segments were successively deactivated according to the feed rate. The second stage was the cooling phase, which was implemented by convective heat flux. The analysis of FE-simulation showed the major influence of geometry discretization and the time stepping parameters on the precision of the finite element model.

Tai et al. (2012) demonstrated that for deep-hole drilling, heat sources on the whole wall surface can be significant due to friction between drill margins and workpiece, chip accumulated in the drill for evacuation and heat transfer from high temperature drill to workpiece. They developed a method that uses the advection model of Bono and Ni to determine the heat flux in bottom surface and another simulation to separately find the heat input on the whole wall surface. The results showed that as the drilling depth increases the heat power on whole wall surface becomes more significant. Although the good results, this method needs of temperature measurements very close to the hole what can be a difficult experiment and uses a combination of simulations to determine the two heat fluxes separately what can generated a high computational cost.

The estimation of a heat flux distribution or the temperature gradient using a measured temperature history inside a solid is called the inverse heat conduction problem (IHCP). This type of problem is usually unstable because the solutions and parameters have to be determined from indirect observable data which contain measurement error. Various different methods, including analytical and numerical approaches, have been developed to handle the IHCP in one, two and three-dimensional domains.

The inverse problem is based on the minimization of error between a measured and a calculated temperature. An inverse analytical approach was used by Battaglia et al. (2005) to estimate the temperature, they did stationary and linearity assumptions to break down the 3D problem in a 2D problem. Some of the methods commonly used are: the least squares method (Cui et al., 2012), the conjugate gradient method (Lu et al., 2012), the function specification method (Blanc et al., 1998), genetic algorithms (Gosselin et al., 2009) and neural networks (Deng and Hwang, 2006).

The application of the PSO to solve the inverse heat conduction problem wasn't very much studied, maybe because is a relatively new optimizer. The effectiveness and efficiency of PSO in inverse conduction problems were studied by Vakili and Gadala (2009). Three variations of PSO were used to solve boundary inverse heat conduction problem in one, two and three dimensions, in steady and transient problems. The results show that PSO can be successfully applied with a good efficiency improvement, compared to a genetic algorithm, especially in more complex test cases. Moreover it was also presented that the stability problem of the classical inverse approaches in dealing with smaller time steps can be mitigated in PSO. Liu (2012) also used PSO-based algorithms in an inverse analysis of surface heat flux for three-dimensional heat conduction. It was presented three different modifications in the PSO algorithm and some of the modifications resulted in performance improvement.

Evolutionary computational techniques work on a population of potential solutions on a search space. The particle swarm optimization was first designed and developed by Kennedy and Eberhart (1995) based on the social behavior theory. It was proposed a method for optimization of continuous nonlinear functions. The PSO algorithm is initialized with a random potential solutions and each one of these "solutions" is named as particle. Each particle is a

point in a D-dimensional space, where D is the number of dimensions each particle has and the dimensions are the number of variables that are being optimized. The *i*th particle is represented as $X_i = (x_{1D}, x_{2D}, ..., x_{iD})$ and these particles are manipulated according to Eq. 1 and 2:

$$v_{iD} = v_{iD} + \phi_p * r_p * (p_{iD} - x_{iD}) + \phi_g * r_g * (g - x_{iD}) \quad (1)$$

$$x_{iD} = x_{iD} + v_{iD} \quad (2)$$

where the best previous position is recorded and presented as $P_i = (p_{1D}, p_{2D}, ..., p_{iD})$. The best particle among all the particles in the population is represented by the symbol g and the velocity (position change) rate for particle i is represented as $V_i = (v_{1D}, v_{2D}, ..., v_{iD})$, ϕ_p and ϕ_g are two constants and r_p and r_g are two random functions in the range [0,1].

Equation 1 is used to calculate the particles new velocity according to its previous velocity and the distances of its current position from its own best position and the group's best position. Then the particle is moved to a new position according to Eq. 2. The performance of each particle is measured according to a predefined fitness function, which is related to the problem to be solved.

The second and the third parts of the velocity equation Eq. 1 have the objective to change the velocity particle. Without these two parts, the particles would keep in the same direction at the current speed until hit the boundary. The second part is the cognitive part, which represents the particle own history and the third part is the social part, which represents the collective history of the swarm when searching. If ϕ_p is equal ϕ_g then the particle will search equally with cognitive and social parts, however when one of the constants is bigger than other the particle will tend to use more of the related history (Li and Qu, 2012).

A new version of particle swarm optimization was developed after the addition of a new inertia weight. The inertia weight ω is brought into the Eq. 1 that is transformed in the Eq. 3 and plays the role of balancing the global search and the local search. It can be a positive constant or even a positive linear or nonlinear function of time (Shi and Eberhart, 1998). A large inertia weight facilitates the global search while a small inertia weight facilitates the local search.

$$v_{iD} = \omega * v_{iD} + \phi_p * r_p * (p_{iD} - x_{iD}) + \phi_g * r_g * (g - x_{iD}) \quad (3)$$

One of the parameters of the PSO is the number of particles (S), also called swarm or population. The influence of this parameter was studied by some researchers. Shi and Eberhart (1999) did an experimental study using the PSO and the results showed that its performance wasn't sensitive to the swarm size. The convergence analysis performed by Trelea (2003) demonstrated that in most of cases, increasing the number of particles decreased the number of required algorithm iterations. The success rate was also increased significantly. On the literature there isn't a definition about the ideal number of particles in the swarm.

The main objective of PSO is to minimize an objective function that was predefined, usually an error function. The main objective of PSO is to minimize an objective function that was predefined and the iterative process can be visualized in Fig. 2. The iterative process is initialized with a swarm of S random particles' positions is generated, and the value of x_{iD} is a number between 0 and 1. Each particle has a number D of dimensions, that is the number of variables that are being optimized and each one of these variables have lower and upper bounds. When the particle has a position $x_{iD} = 0$ each variable will have the lower bound value and if a particle has position $x_{iD} = 1$ the variable will have the upper bound value.

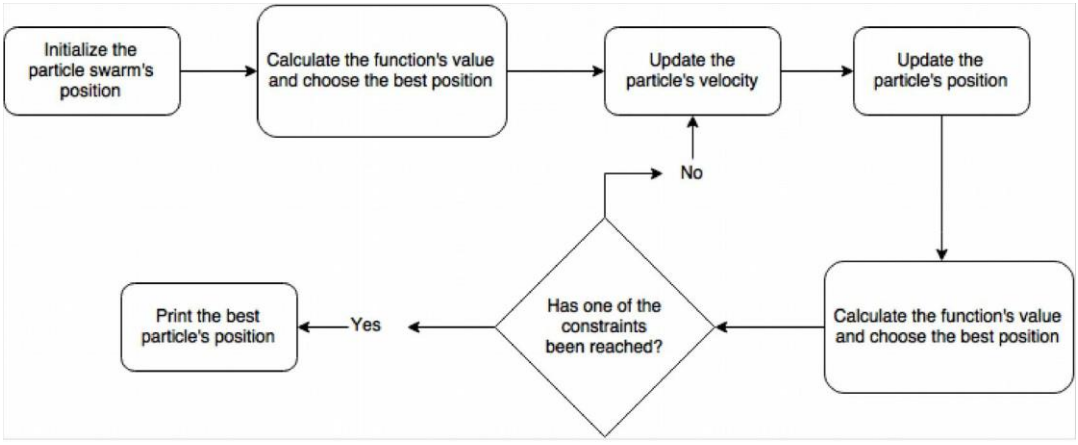

Figure 2: PSO diagram

The objective function's value to each particle is calculated and the position of the particle with the best result is stored. The particle's velocity is then randomly calculated and updated. Then a new swarm is randomly generated according to Eq. 3 and Eq. 2, the objective function's value is calculated and if a better result is found the respective particle's position is stored.

The search for a best particle's position is ended if one of the defined constraints has been reached. The three constraints used are: if the function's value change is less than a predefined value, or if the position change is less than a predefined value, or if the maximum number of iterations without find a best function's value is reached.

2. MATERIALS AND METHODS

2.1. Experimental Tests

An experimental study was performed using a 10.5 mm diameter and 140 mm long drill. A hole, 50 mm in depth, was drilled in the center of a cylindrical workpiece, 43 mm in diameter and 60 mm in length. The work material is SAE 1020 steel with 7832 kg/m density, 52 W/m-K thermal conductivity and 434 J/Kg-K specific heat.

Five type K thermocouples were embedded in the workpiece, their positions were distributed along the plate length as: T1 = 10 mm, T2 = 20 mm, T3 = 30 mm, T4 = 40 mm and T5 = 50 mm, being zero the top surface of the workpiece. The thermocouple hole was 3 mm and filled with a high thermal conductivity paste to minimize the thermal resistance. The temperatures were recorded at a 100 Hz sampling rate using a National Instruments Module. The dry drilling process was performed in a CNC lathes ROMI D600. The cutting conditions used in the operation are: V_c = 40 m/min and f = 0.2 mm/rot.

2.2. Heat Transfer Problem

The FEM model and the inverse procedure are focused on predicting the heat flux to workpiece (Q_{wp}) generated during the drilling operation (Fig. 1). But firstly an analytical model of the problem must be presented. The heat balance of the workpiece comes from the first law of thermodynamics, which can be summarized as conservation of energy.

$$\dot{E}_i - \dot{E}_{out} + \dot{E}_{gen} = \dot{E}_{stor} \tag{4}$$

where E_i is the energy entering in control volume, E_{out} is the energy that is exiting the control volume, E_{gen} is the energy generated and E_{stor} is the energy stored in the control volume.

Considering the energy balance equation, we can define the heat conduction entering in control volume as Q_x and Q_y in the directions x and y. The control volume has dimensions of dx and dy. The rates of heat conduction are defined as:

$$\dot{Q}_x = -k\, dy \frac{\partial T}{\partial x} \tag{5}$$

$$\dot{Q}_y = -k\, dx \frac{\partial T}{\partial y} \tag{6}$$

Here, k is the thermal conductivity of the workpiece material, and dy is the surface that is exposed to this heat conduction from direction x and dx is the surface relative to heat conduction in direction y. The heat conduction rates exiting the control volume from x and y directions can be found from Taylor series expansion of the derivative of heat conduction rates and ignoring higher order terms:

$$\dot{Q}_{x+dx} = \dot{Q}_x + \left(\frac{\partial \dot{Q}_x}{\partial x} dx \right) \tag{7}$$

$$\dot{Q}_{y+dy} = \dot{Q}_y + \left(\frac{\partial \dot{Q}_y}{\partial y} dy \right)$$

(8)

These equations involve only the heat conduction terms. Since the study is two-dimensional, and the system is stationary with air flowing around, there is heat loss by convection from the workpiece. This heat convection is included in the model as exiting the control volume to the surroundings, if the control volume in consideration has contact with surroundings. Therefore, this heat convection rate is directed from the control volume to the surrounding air:

$$\dot{Q}_{conv} = h dx dy \left(T - T_{\infty}\right) \tag{9}$$

where h is the convection coefficient between the workpiece and the ambient air flowing around. These terms become zero if the control volume is not in contact with air.

The energy generated is equal to the heat generation rate times the area of the control volume, but if the control volume is not in the heat generation zone the term becomes zero. The amount of heat stored within the control volume is related to the density ρ, specific heat capacity c_p and the rate of change in temperature.

$$\dot{E}_{gen} = \dot{Q}\, dx dy \tag{10}$$

$$\dot{E}_{stor} = \rho C_p \frac{\partial T}{\partial t} dx dy \tag{11}$$

As the maximum temperature measured isn't higher than 50 ºC. Then the thermal properties, thermal conductivity, film condition and specific heat, are considered constant with values: $k = 52.0$ *W/mK*, $h = 10$ *W/m*^{2}*K* and $C_p = 434$ *J/KgK*. The radiation heat transfer is not considered in this analysis. Then the heat balance equation in the control volume can be written as:

$$\dot{Q}_x + \dot{Q}_y - \dot{Q}_{x+dx} - \dot{Q}_{y+dy} - \dot{Q}_{conv} + \dot{Q}\, dx dy = \rho C_p \frac{\partial T}{\partial t} dx dy \tag{12}$$

The equation still can be simplified, the dimensional heat conduction rates become second derivatives of temperature with corresponding dimension and if we divide both sides by ($kdxdy$) then the heat balance equation is:

$$\frac{\partial^2 T}{\partial x^2} + \frac{\partial^2 T}{\partial y^2} + \frac{\dot{Q}}{k} - \frac{h\left(T - T_{\infty}\right)}{k} = \frac{\rho C_p}{k} \frac{\partial T}{\partial t} \tag{13}$$

2.3. Heat Generation

The term of heat generation in the Eq. 13 is the fraction of heat generated in the process that is transferred to workpiece. Assuming that all the energy in the cutting process is transformed into heat, the total heat can be calculated by the Eq. 14:

$$Q_{total} = 2 \times \pi \times M \times \frac{n}{60} \times t_c \tag{14}$$

where M is the experimentally measured drilling torque, n is the rotation speed of the drill and t_c is the machining time. However, as previously presented the heat input into workpiece (Q_{wp}) can occur in two of the three heat generation zones: the primary zone that is the tool bottom surface (Q_{wp1}) and the secondary zone that is the just-machined hole wall (Q_{wp2}), then just a portion of the heat generated is conducted to workpiece and it can be said that $Q_{wp} = Q_{wp1} + Q_{wp2}$.

The dimensions of the hole studied in the research are $D_h = 10.5$ *mm* and $L_h = 50$ *mm*. The heat flux in this research is considered as a spatial and time distribution along the hole wall. The distribution used is defined as in Fig. 3

with a uniform distribution of length a and Q_{max} linear distribution from Q_{max} until zero with length from a until the workpiece top surface. The heat source moves with a velocity according to feed rate, that in this study is $V_f = 0.242$ *m/s*.

2.4. Finite Element Model

The finite element analysis of the workpiece temperature was performed using ABAQUS 6.12. Figure 4 shows the two-dimensional axisymmetric mesh used in this study. Diameters of the workpiece and drill are denoted as D_w and D_d. The length of workpiece and the hole drilled are denoted as L and l. Four-node linear axisymmetric element (DCAX4) was selected in this study. The hole was considered already drilled and the heat source was applied in the hole wall trough the subroutine *Dflux*.

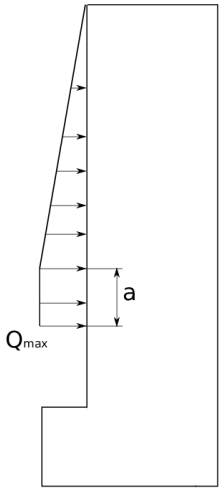

Figure 3: Heat flux distribution

This type of mesh was chosen because of the geometrical conditions. The workpiece is a cylinder that can be represented by a rectangular section, the initial and load conditions are symmetric. The simulation was performed in two steps, the drilling phase and the cooling phase.

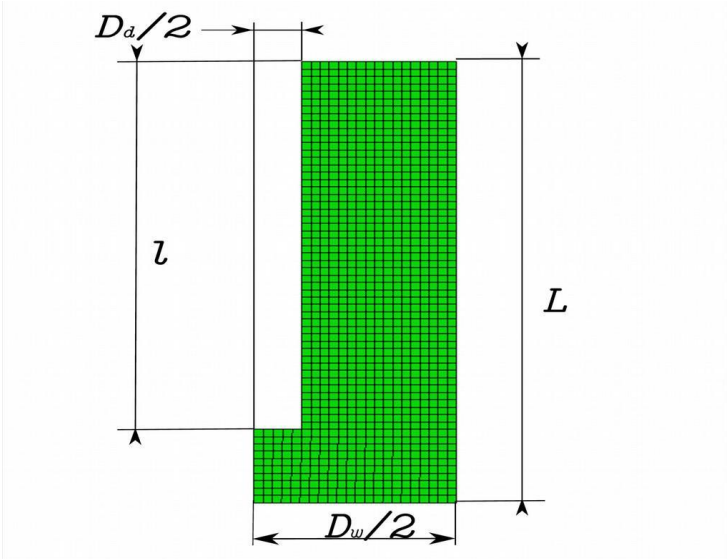

Figure 4: 2-D axisymmetric finite element mesh

2.5. Mesh refinement

The influence of the finite element parameters as element size and time integration were analyzed before the iterative analysis to identify the heat flux. The mesh refinement was done with a heat source defined by a uniform part and a linear part. The element sizes used in the simulations were $S_1 = 2.5$ *mm*, $S_2 = 1$ *mm*, $S_3 = 0.5$*mm* and $S_4 = 0.25$*mm*.

These sizes were chosen because the temp points analyzed can be the same in the experimental tests. In these analyzes were used the time steps $\Delta_{t,d} = 0.1s$ and $\Delta_{t,c} = 2.0\ s$. The difference in the maximum temperature between the different element sizes was less than *1 %*. Because of this, the influence of this parameter is insignificant and then the S_2 element size was chosen.

The step time influence was analyzed separately in drilling and cooling phase. In drilling phase the time step was chosen based in the total drilling time, that is 12,4 s. The first step time used was the time required for the tool to drill 2 mm. This step time is $\Delta_{t,d\_1} = 496\ ms$, the other step times were defined as $\Delta_{t,d\_1}/2$, $\Delta_{t,d\_1}/4$, $\Delta_{t,d\_1}/8$ and $\Delta_{t,d\_1}/16$. In these analyzes the other parameters were $S = 1\ mm$ and $\Delta_{t,c} = 2.0\ s$. In the time discretization of the first step, the maximum temperature variation decreases as step time decreases. The defined step time was $\Delta_{t,d} = 62\ ms$, because reducing the time step to $\Delta_{t,d} = 31\ ms$ resulted in a relative decrease of less than 1%.

In the cooling phase five different time steps were analyzed. The first step time used was $\Delta_{t,c\_1} = 10.0\ s$ and the others step times were defined as: $\Delta_{t,c\_1}/2$, $\Delta_{t,c\_1}/5$, $\Delta_{t,c\_1}/10$ and $\Delta_{t,c\_1}/20$ The shorter the time step the higher the temperature variation in the workpiece. The temperature increment between the time steps $\Delta_{t,c}$ = 1.0s and $\Delta_{t,c}$ = 0.5s was only 1%, but the computer time required was increased in more than 50 % because of this 1.0 was defined as an appropriated time step to this phase.

2.6. Inverse Procedure

The inverse procedure used in this study consists of the minimization of the average error between the experimental and the numerical results. The error function is defined by:

$$err_{av} = \sum_{i=1}^{I} err_i / I \tag{16}$$

where I is the number of input points of temperature, T_{inexp} and T_{insim} are the measured and simulated temperatures at the input point, and N is the number of temperature points at each input used in error calculation. The number of temperature points varies according to each input point. The input points in this study are the same location of the thermocouples used in experimental tests.

The inverse procedure in this study uses a particle swarm optimization algorithm to determine the heat flux parameters of each distribution. The PSO parameters and their influence in the optimization process were presented. The parameters chosen in this study can be seen in Tab. 1. The one parameter that changes at the different analyzes is the swarm size (S) that is related to the number of dimensions of each different distribution analyzed.

Table 1. PSO parameters used in the inverse procedure.

PSO Parameters	
Swarm size (S)	10
Inertial weight (ω)	0.5
Cognitive factor (ϕ_g)	0.5
Social factor (ϕ_p)	0.5
Maximum number of iterations	20
The minimum position changes	10^{-8}
The minimum objective value changes	10^{-4}

3. RESULTS

In the first analysis, a heat flux distribution with a uniform and a linear part was considered. In this distribution, the coefficients of Q_{wp} are a and Q_{max}. They are determined through the inverse approach that was previously presented. The values found to the coefficients are $Q_{max} = 452367.2\ W/m^2$ and $a = 0.0073\ m$ with an average error $err_{av} = 7.69\ \%$.

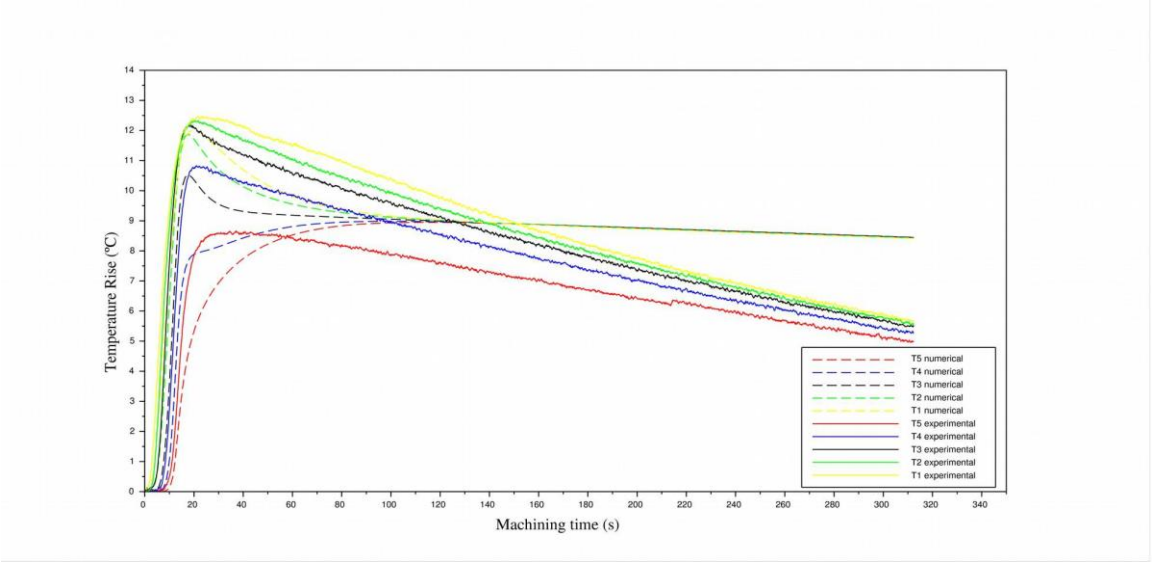

Figure 5: Comparison between the simulated and experimental temperatures in all input points

Figure 5 compares the numerical solution of the workpiece temperature with the experimental results. The maximum temperature decreases due to the heat flux distribution. The superior section of the workpiece is exposed to the maximum heat flux Q_{max} for a longer time than the other sections. The results show different discrepancies to each of the measured point. This can be better analyzed when they are presented separately.

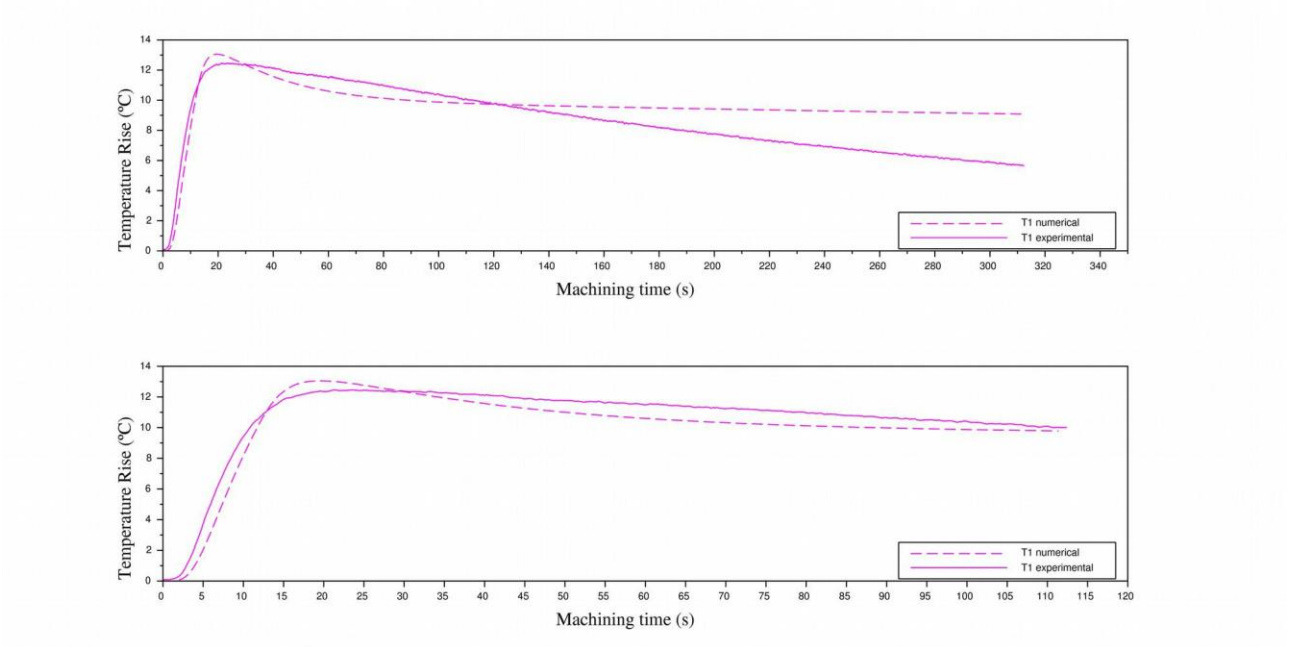

Figure 6: Numerical and experimental temperatures in T1

Analyzing the temperature curve in the input point T1, if we compare the analysis only until *100 s*, it can be seen that the error is less in the beginning than in the end of the analysis. In the cooling step is considered only the convective flux of $h = 10\ W/m^2K$, but the difference in the temperature variation, between the numerical and experimental results in this phase, may be a consequence of heat loss by other sources that were not considered.

It is also evident the difference between the input points. Comparing the temperature curves between *T1 (10 mm)* and *T4 (40 mm)*, the results show better accuracy for *T1*. This effect can be explained because the higher the point is located, remembering that machining begins in the top of workpiece, less sensitive it is to the heat generated in the secondary heat zone (Q_{wp2}). The temperature in input point *T4* has not a good accuracy due to the fact that this portion

of heat is not properly described in the model. This shows that this kind of distribution has a limitation to properly simulate the total heat input to workpiece. The same effect is observed comparing the temperatures between *T2* and *T5*.

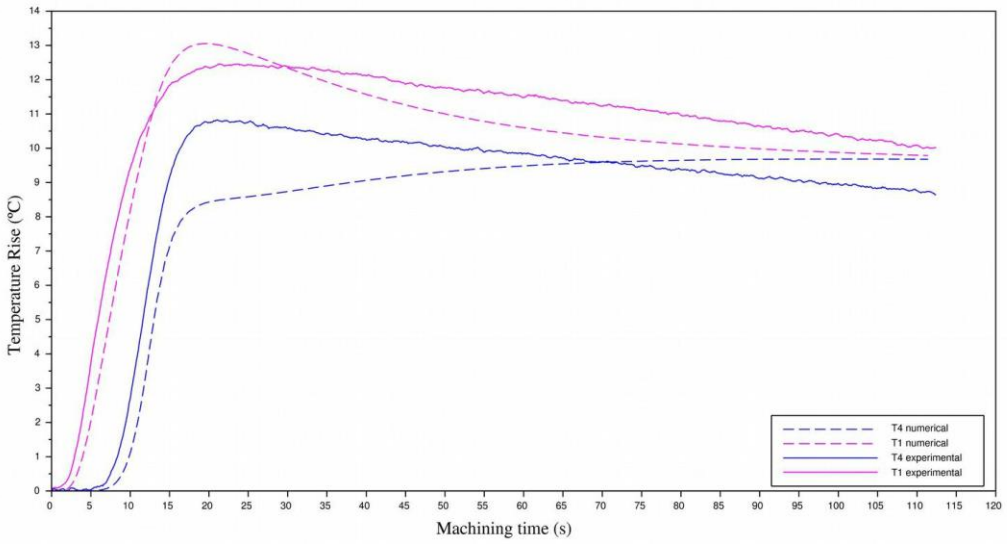

Figure 7: Comparison between temperatures T1 and T4

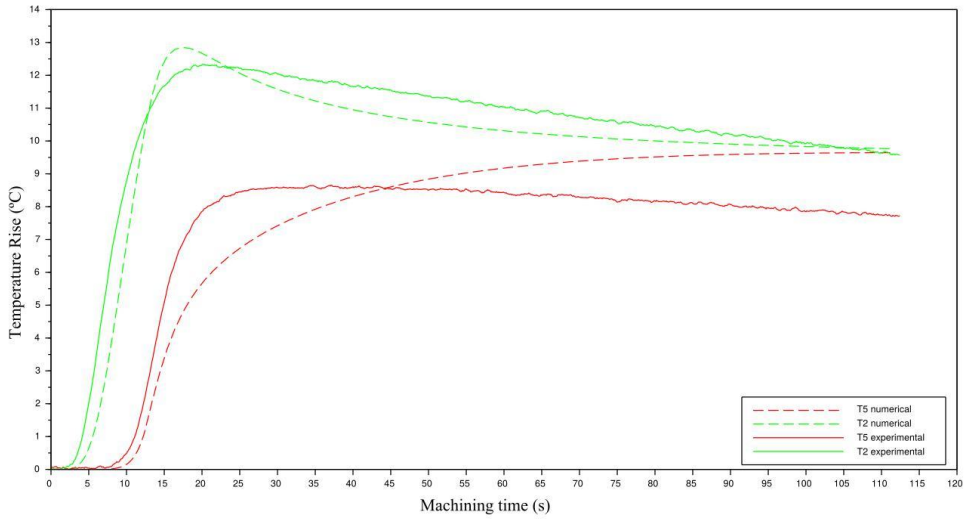

Figure 8: Comparison between temperatures in T2 and T5

4. CONCLUSIONS

The magnitude and the distribution of heat flux transferred to workpiece have been determined using the method based on particle swarm optimization. This method and the proposed distribution was satisfactory to fit the temperature curves in the first points of the analysis, that points that are close to the beginning of drilling process. The model can be used in different cutting conditions, it just need to adapt the dimensions of the geometric model used to generate the finite element model and the feed rate (V_f) that defines the heat source movement.

The increase of the error in the input points located in the lower regions of workpiece demonstrates that this kind of distribution is limited in the representation of the heat generated in the secondary heat zone. Although the study

done in this paper focus in the drilling process, this can be easily adapted to other machining process as milling and turning. It just needs to adapt the distribution of heat flux to workpiece.

5. REFERENCES

Battaglia, J.; Puigsegur, L. and Cahuc, O. “Estimated temperature on a machined surface using an inverse approach”. Experimental heat transfer, Taylor & Francis, v. 18, n. 1, p. 13–32, 2005.

Ber, A. and Goldblatt, M. “The influence of temperature gradient on cutting tool’s life”. CIRP Annals-Manufacturing Technology, Elsevier, v. 38, n. 1, p. 69–73, 1989.

Biermann, D. and Iovkov, I. “Modeling and simulation of heat input in deep-hole drilling with twist drills and mql”. Procedia CIRP, Elsevier, v. 8, p. 88–93, 2013.

Blanc, G.; Raynaud, M. and Chau, T. H. “A guide for the use of the function specification method for 2d inverse heat conduction problems”. Revue générale de thermique, Elsevier, v. 37, n. 1, p. 17–30, 1998.

Bono, M. and Ni, J. “A model for predicting the heat flow into the workpiece in dry drilling". Journal of Manufacturing Science and Engineering, American Society of Mechanical Engineers, v. 124, n. 4, p. 773–777, 2002.

Cui, M.; Gao, X. and Zhang, J. “A new approach for the estimation of temperature- dependent thermal properties by solving transient inverse heat conduction problems”. International Journal of Thermal Sciences, Elsevier, v. 58, p. 113–119, 2012.

Deng, S. and Hwang, Y. “Applying neural networks to the solution of forward and inverse heat conduction problems”. International Journal of Heat and Mass Transfer, Elsevier, v. 49, n. 25, p. 4732–4750, 2006.

Fleischer, J.; Pabst, R. and Kelemen, S. “Heat flow simulation for dry machining of power train castings”. CIRP Annals- Manufacturing Technology, Elsevier, v. 56, n. 1, p. 117–122, 2007.

Gosselin, L.; Tye-Gingras, M. and Mathieu-Potvin, F. “Review of utilization of genetic algorithms in heat transfer problems”. International Journal of Heat and Mass Transfer, Elsevier, v. 52, n. 9, p. 2169–2188, 2009.

Kennedy, J. and Eberhart, R. “Particle swarm optimization”. In: Proceedings of 1995 IEEE International Conference on Neural Networks. [S.l.: s.n.], 1995. p. 1942–1948.

Li, Z. and Qu, X. L. “The novel parameter selection of particle swarm optimization”. In: TRANS TECH PUBL. Advanced Materials Research. [S.l.], 2012. v. 479, p. 344–347.

Liu, F.B. “Particle swarm optimization-based algorithms for solving inverse heat conduction problems of estimating surface heat flux”. International Journal of Heat and Mass Transfer, Elsevier, v. 55, n. 7, p. 2062–2068, 2012.

Lu, S.; Heng, Y. and Mhamdi, A. “A robust and fast algorithm for three-dimensional transient inverse heat conduction problems”. International Journal of Heat and Mass Transfer, Elsevier, v. 55, n. 25, p. 7865–7872, 2012.

Segurajauregui, U.; Arrazola, P. J. Heat-flow determination through inverse identification in drilling of aluminium workpieces with mql. Production Engineering, Springer, v. 9, n. 4, p. 517–526, 2015.

Shi, Y. and Eberhart, R. “A modified particle swarm optimizer”. In: IEEE. Evolutionary Computation Proceedings, 1998. IEEE World Congress on Computational Intelligence., The 1998 IEEE International Conference on. [S.l.], 1998. p. 69–73.

Shi, Y. and Eberhart, R. C. “Empirical study of particle swarm optimization”. In: IEEE. Evolutionary Computation, 1999. CEC 99. Proceedings of the 1999 Congress on. [S.l.], 1999. v. 3.

Tai, B. L.; Stephenson, D. A. and Shih, A. J. “An inverse heat transfer method for determining workpiece temperature in minimum quantity lubrication deep hole drilling”. Journal of Manufacturing Science and Engineering, American Society of Mechanical Engineers, v. 134, n. 2, p. 021006, 2012.

Tay, A. “A review of methods of calculating machining temperature”. Journal of Materials Processing Technology, Elsevier, v. 36, n. 3, p. 225–257, 1993.

Tay, A.; Stevenson, M. and Davis, G. D. V. “Using the finite element method to determine temperature distributions in orthogonal machining”. Proceedings of the institution of mechanical engineers, SAGE Publications, v. 188, n. 1,p. 627–638, 1974.

Taylor, F. W. “On the art of cutting metals”. New York, The American Society of Mechanical Engineers, [1907], 1907.

Trelea, I. C. “The particle swarm optimization algorithm: convergence analysis and parameter selection”. Information processing letters, Elsevier, v. 85, n. 6, p. 317–325, 2003.

Vakili, S. and Gadala, M. “Effectiveness and efficiency of particle swarm optimization technique in inverse heat conduction analysis”. Numerical Heat Transfer, Part B: Fundamentals, Taylor & Francis, v. 56, n. 2, p. 119–141, 2009.

RESPONSIBILITY NOTICE

The authors are the only responsible for the printed material included in this paper.